Biophysical Chemistry 136 (2008) 101–107

Contents lists available at ScienceDirect

Biophysical Chemistry

journal homepage: http://www.elsevier.com/locate/biophyschem

Cadmium sulfide-modified GCE for direct signal-amplified sensing of DNA hybridization

Qing Xia [a,b], Xing Chen [a], Jin-Huai Liu [a,b,*]

[a] Key Laboratory of Biomimetic Sensing and Advanced Robot Technology, Anhui Province, Institute of Intelligent Machines, Chinese Academy of Science, Hefei, 230031 Anhui, PR China
[b] Department of automation, University of Science and Technology of China, Hefei, 230026 Anhui, PR China

ARTICLE INFO

Article history:
Received 19 February 2008
Received in revised form 6 May 2008
Accepted 6 May 2008
Available online 17 May 2008

Keywords:
DNA hybridization
CdS-ODN nanoparticles
Cyclic Voltammogram
Differential Pulse Voltammogram

ABSTRACT

A novel DNA hybridization sensor based on nanoparticle CdS modified glass carbon electrode (GCE) was constructed and characterized coupled with Cyclic Voltammogram (CV) and Differential Pulse Voltammogram (DPV) techniques. The mercapto group-linked probe DNA was covalently immobilized onto the CdS layer and exposed to oligonucleotide (ODN) target for hybridization. The structure of DNA sensor was characterized by X-ray diffraction (XRD), field-emission microscopy (FESEM) and X-ray photoelectron spectra (XPS). Sensitive electrical readout achieved by CV and DPV techniques shown that when the target DNA hybridized with probe CdS-ODN conjugates and the double helix formed on the modified electrode, a significant increased response was observed comparing with the bare electrodes. The selectivity of the sensor was tested using a series of matched and certain-point mismatched sequences with concentration grads ranging from 10^{-6} μM to 10^{1} μM. The signal was in good linear with the minus logarithm of target oligonucleotide concentration with detection limit <1 pM and the optimized target DNA concentration was 10^{-6} μM for the signal amplification. Due to great surface properties, the additional negative charges and space resistance of as-prepared CdS nanoparticles, the sensor was able to robustly discriminate the DNA hybridization responses with good sensitivity and stability.

1. Introduction

In recent years, major developments in human genetics research have desperate demands for rapid, handy and sensitive biosensors to realize the real-time detection of gene expression process and the measurement of gene expression products. An effective DNA-sensing system provides a potential use in a variety of fields, such as biomedical engineering, clinical diagnosis, food development and environmental protection. Various techniques including radiochemical, colorimetric, acoustic, chemiluminescent methods [1–3] have been employed as readout modalities. The demand for one-step label-free gene detection has aroused extensive researches on attractive electrochemical method which combines biochemical, medical and electronic techniques with the advantages of being cheap, reliable, sensitive, selective and miniaturizing [4]. DNA hybridization sensors rely on highly specific recognition process between a target analyte and a probe that is closely connected or integrated within a transducer to provide a detectable readout of the redox indicator, including metal complexes [5], organic intercalating compounds [6], nanotubes [7] and enzyme labels [8–10]. However, transduction and signal amplification of the hybridization signals have proven to be challenging. The unique electrical and bio-compatible nanometer sized particles (NPs) such as gold and silver are demonstrating excellent prospects [11]. Besides those applications, the increased sensitivity of these sensors typically results from the magnetic and amplifications that effectively concentrates semiconductor quantum dots (such as CdS and ZnS) as ODN labeling tags on the electrode for detection of DNA hybridization [12,13]. The reported steps involved conducting polymers (CP) as a versatile substrate which can covalently attach short ODNs to the polymer chains [14–16] and the electronic structure caused by the presence of the bioprobe/target conjugate leading to a change in macroscopic material properties [17,18].

In this article, a kind of novel cadmium sulfide (CdS) nanoparticles with special walnut-like surface is synthesized by solvothermal method which can firmly attach onto the surface of electrode directly and covalently bind with mercapto group modified probe ssDNA to produce DNA-ODN conjugates as reported [19]. We illustrate the signal enhancement resulting from nanoparticle labeling comparing with the unlabelled ones and the mechanisms by which target DNA concentration related response changes occurred via Cyclic Voltammogram (CV) and Differential Pulse Voltammogram (DPV) techniques have been elaborated in details.

2. Experimental

2.1. Reagents and Apparatus

Cadmium chloride ($CdCl_2$•$2.5H_2O$, AR), sodium thiosulfate pentahydrate ($Na_2S_2O_3$•$5H_2O$, AR), poly (*N*-vinyl-2-pyrrolidone) (PVP, K30) and

* Corresponding author. Key Laboratory of Biomimetic Sensing and Advanced Robot Technology, Anhui Province, Institute of Intelligent Machines, Chinese Academy of Science, Hefei, 230031 Anhui, PR China. Tel.: +86 551 5591142; fax: +86 551 5592420.
E-mail address: jhliu@iim.ac.cn (J.-H. Liu).

0301-4622/$ – see front matter © 2008 Elsevier B.V. All rights reserved.
doi:10.1016/j.bpc.2008.05.002

absolute ethanol were purchased from Sangon Bioengineering Ltd. Company (Shanghai, China) without further purification unless indicated. The various oligonucleotides purchased from Sangong Bioengineering Ltd. Company (Shanghai, China) have the following sequences:

Probe DNA 5′-SH-AGGCTCCTGGCGCACT-3′
- complementary (target) DNA 5′-AGTGCGCCAGGAGCCT-3′
- one-point mismatch target 5′-AGCGCGCCAGGAGCCT-3′
- two-point mismatch target 5′-AGCCCGCCAGGAGCCT-3′

All the stock solutions of ODNs were prepared with TE solution: 0.1 M Tris–HCl buffer +1.0 mM EDTA (pH 7.6) and kept frozen until used. Other reagents were commercially available and all of analytical reagent grade.

2.2. Cadmium sulfide synthesis

0.5 mmol Cadmium chloride ($CdCl_2$•$2.5H_2O$, AR) and 0.5 mmol sodium thiosulfate pentahydrate ($Na_2S_2O_3$•$5H_2O$, AR) were dissolved in 30 ml distilled water under vigorously stirring for 15 min, then 0.12 g PVP was introduced into the above solution under continuous stirring for 15 min, resulting in a clear and colorless solution. The solution and 20 ml distilled water were transferred into Teflon liner autoclave with 50 ml capacity. The autoclave was sealed and maintained at 160, for 12 h, then cooled naturally to room temperature. Finally, the precipitates were dispersed in absolute ethanol.

2.3. Characterizations of CdS-ODN conjugate

SEM images of CdS nanoparticles were taken by field-emission microscopy (FESEM, Sirion 2000, 5 kV). The products dispersed in absolute ethanol were characterized by X-ray diffraction (XRD) using a Philips X'Pert Pro MPD X-ray diffractormeter equipped with monochromatic high-intensity CuKα radiation (λ = 1.542512 nm). X-ray photoelectron spectroscopy (XPS) measurement was performed on an ESCALAB MK II spectrometer (VG Co., United Kingdom) with Al Ka X-ray radiation as the X-ray source for excitation and analyzer pass energy of 20.0 eV. Typically, the limited operating pressure in the analysis chamber was $\leq 2.0\times10^{-10}$ Pa. The resolution of the spectrometer was 0.9 eV.

2.4. GCE pretreatment

The GCE was polished with 0.05 μm alumina slurry, sonicated in absolute ethanol, 1.0 M HCl and deionization water for 5 min, respectively.

2.5. Modification of GCE with PVP-capped CdS nanoparticles

As-prepared CdS nanoparticles were diluted into solution (1.16×10^{-6} M) and ultrasonic dispersed. Then 5 μL the solution was dropped onto the GCE surface and dried in the air.

2.6. Preparation of CdS-DNA nanoconjugates on the surface of GCE

Mercapto group modified probe DNA 5 μL was dripped onto the CdS-modified GCE surface rinsed with deionization water and dried first to form the nanoconjugates at 20.

2.7. Hybridization of target DNA with probe DNA on the surface of GCE

Different concentrations (10^{1} μM, 10^{0} μM, 10^{-1} μM, 10^{-2} μM, 10^{-3} μM, 10^{-4} μM, 10^{-5} μM, 10^{-6} μM) of target DNA including complementary, one-point mismatched and two-point mismatched 5 μL respectively were added onto the surface of GCE to get a serious of GCE samples. The hybridization reaction was carried out at 20, for 2 h. The obtained GCE samples were rinsed with 0.1 M Tris–HCl buffer to remove excess ODN probes, and then dried in the air.

2.8. Electrochemical detection

Cyclic Voltammogram (CV) measurements were performed in a 0.1 M PBS buffer solution (with 0.1 M NaCl, pH 7.0) containing a 0.01 M $K_3[Fe(CN)_6]$ solution which seemed as a redox marker and operated from −0.5 V to 1.0 V (vs. Ag/AgCl) with scan rate 50 mV/s. Differential Pulse Voltammogram (DPV) measurements were also performed in the same experimental condition with potential intervals from 0.2 V to 0.9 V, pulse amplitude 25 mV, pulse width 60 ms and scan rate 20 mVs^{-1}. Cycle Voltammetry (CV) scans was performed with a LK 2005 electrochemical analyzer (Lanlike Instruments Inc. Tianjin, China). The conventional three-electrode electrochemical system consisted of GCE (3 mm diameter) as the working electrode, a platinum slide as the auxiliary electrode and an Ag/AgCl (saturated with KCl) which was used as reference electrode. All potentials mentioned in this paper referred to this reference electrode.

Repetitive measurements were performed by renewing the surface and repeating the above assay preparation procedures. The schematic illustration of the electrochemical detection of DNA hybridization process had been displayed in Scheme 1.

3. Results and discussion

3.1. Sensor construction

Fang's group [19] had demonstrated that a type of cadmium sulfide (CdS) nanoparticles coated with free carboxyl groups on the surface was directly synthesized in aqueous solution, which could covalently bind with the amine modified probe DNA to produce CdS-DNA nanoconjugates. As shown in Scheme 1, we had used a similar method to produce DNA sensor based on CdS-modified GCE. In the configuration investigated in this paper, as-prepared CdS nanoparticles which have great superficial properties are attached onto the surface of GCE to effectively covalently bind the mercapto group modified probe DNA. The resulting sensor therefore allows the detection of hybridization with complementary and mismatched target DNA.

3.2. Structure of as-prepared CdS nonoparticles

From Fig. 1, the reflection peak can be indexed to hexagonal CdS with lattice constants of α=4.141 Å and c=6.718 Å, which is in great agreement with the literature data (JCPDS card No.41-1049). Compared with the standard card, the relative intensity of peak corresponding to the (100), (002), (101), (110), (112), (202) planes are obvious; the (101) diffraction peak in hexagonal CdS is unusually strong and narrow, which is ascribed to the preferential growth along (101) plane of CdS crystallites. The peak broadening in the XRD patterns clearly indicated the nature of the small-size nanocrystal which demonstrated potential electronic and catalytic properties.

The SEM images in Fig. 2 indicate that the products formed under this dosage of PVP (0.12 g/50 ml) are composed of homogeneous nanopheres with narrow diameter distributions of about 400–500 nm. These nanospheres which have walnut-like surfaces constructed from the assembly of short nanorods and nanoflakes are dispersed with great uniformity. This novel kind of nanoparticles have rough surface which can increase the specific surface area to trap more probe DNA and act as a catalyzer of DNA hybridization.

3.3. XPS system

X-ray photoelectron spectra (XPS) measurements were performed to obtain the elemental composition of the multi-component layers to confirm the immobilization of CdS nanoparticles on the surface of GCE and the covalently bonding of probe DNA to the as-prepared CdS nanoparticles.

X-ray photoelectron spectroscopy is used to ascertain the nature of the functional groups present on the surface of the electrochemically

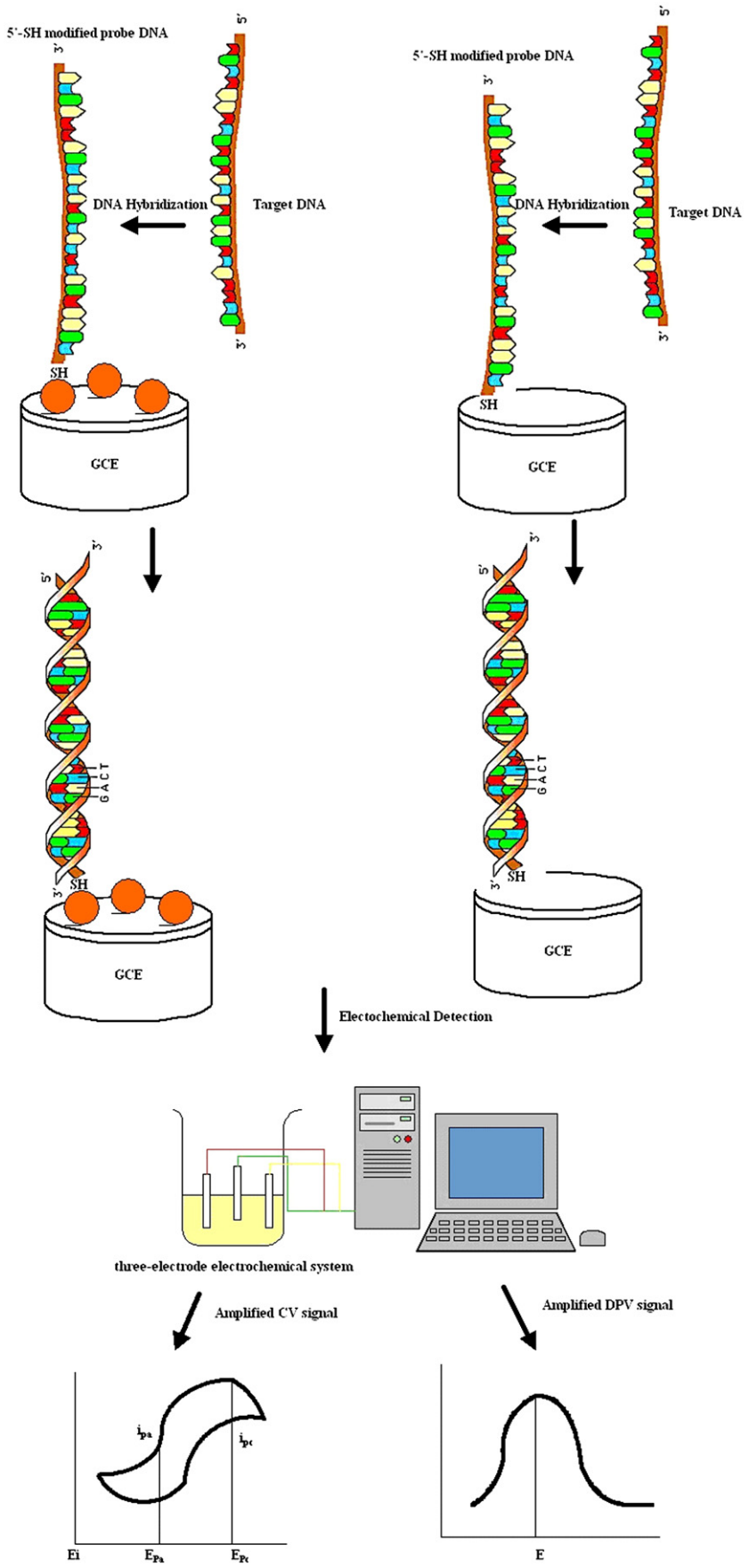

Scheme 1. Process of CdS-modified GCE for the detection of DNA hybridization underlying the sensor response. (Left) Formation of a layer of CdS-ODN nanoconjugates on the surface of GCE before DNA hybridization. (Right) Direct mobilization of ODN on the surface of bare GCE for the detection of DNA hybridization.

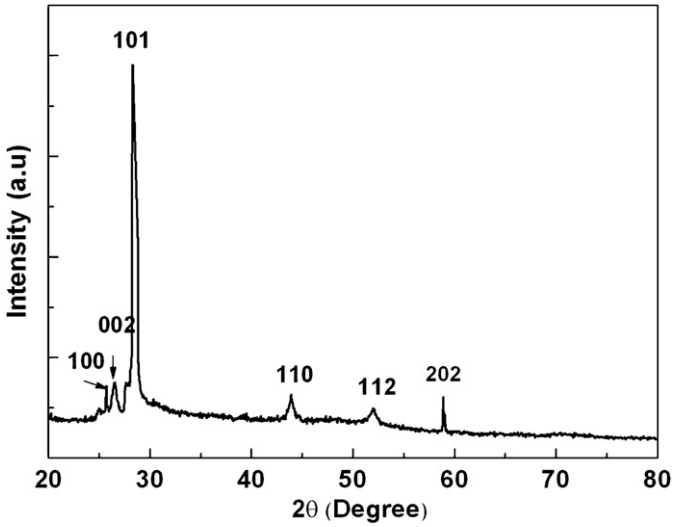

Fig. 1. XRD patterns of CdS crystals obtained under the dosage of PVP 0.12 g/50 ml, the molar ratio of $CdCl_2$•2.5H_2O/$Na_2S_2O_3$•5H_2O=1:1, with reaction for 12 h at 160 °C.

formed layers. Fig. 3(A) shows the wide scan of CdS modified silica (110) after DNA hybridization. The presence of Cd 3d5 with binding energy at 404.79 eV can be cleared observed, indicating CdS had successfully functionalized silica substrates, which means that the surface of GCE can be modified firmly with CdS nonoparticles after rinsing. The N 1s region of the high-resolution XPS spectra acquired for the silica substrate after CdS surface modification step before DNA hybridization in Fig. 3(B) is curve-fitted with three peak energies using multi-peaks Lorentzian approximation. (1) NH_X with binding energy at 399.34 eV; (2) –N–C– with binding energy at 401.24 eV; (3) N–C=O/NH_3^+ with binding energy at 404.86 eV. Collectively, the XPS data confirm that DNA successfully immobilizes onto the surface of CdS modified silica. The content of element Nitrogen which mainly comes from purine bases and pyrimidine bases of nucleotide is treated as a very useful information marker to verify the process of DNA hybridization. After DNA hybridization, the position of the three N 1s peaks are not shifted except for the disappearance of Cd 3d5 peak, which attributes to the overlay of target DNA hybridization with CdS-ODN because the detectable emission electrons without energy loss only come from the sample surfaces with thickness range from 1 to 4 nm or 8 nm. The other peaks shown in the wide scan figure ascribe to the elements came from the TE buffer.

An obvious increase is observed for the nitrogen peak intensities in Table 1. This trend in peak intensity is consistent with the expected overall increase in nitrogen content that accompanied the surface modification steps and process of DNA hybridization resulting from the addition of bases of target DNA. The binding energy of C 1s spectrum decomposes into three components at 284.56, 286.33 and 288.37 eV respectively. The low binding energy (BE) component is assigned to electron emission from the hydrocarbon chains of probe DNA, the sugars and bases in the DNA, while the higher BE component is from the carbons coordinated to the phosphates in the backbone. XPS spectra provides further evidence for the successful DNA hybridization on the CdS modified GCE surface.

3.4. Concentration dependence of the amplified sensor response

Before performing hybridization experiments we examined how incorporation of CdS nanoparticles affected the electrochemical properties of GCE. Fig. 4 curve (a) shows current peak signals of DNA hybridization with CdS modified GCE in a 0.1 M PBS buffer solution (with 0.1 M NaCl, pH 7.0) containing a 0.01 M K_3 [Fe $(CN)_6$] solution which seemed as a redox marker with the concentration of complementary target DNA 10^{-2} μM. The CV of a bare GCE is included for a comparison. It is obvious that peak current in the obtained voltammograms increased with the CdS modified GCE comparing to the bare one. The anode peak potential E_{pc} changes from 0.016 V to 0.083 V and the cathode peak potential E_{pa} 0.452 V to 0.379 V after CdS modification. The potential difference vividly decreases.

In Fig. 5, the peak values decrease when the target DNA concentrations get higher in the concentration range from 10^{-6} μM to 10^{1} μM because the negatively charged PVP-capped CdS nanoparticles (as counter-ions) [12] can attach successfully onto the surface of GCE which has already been confirmed in XPS system above. The intensities of electrostatic repulsion between DNA skeletons and CdS nanoparticles both charged with negative electrons increase with the higher target DNA concentrations.

The ability of the sensor to discriminate between complementary and mismatched oligonucleotides is described as follows: the signal value from the hybridization process for the complementary one is bigger than the mismatched ones under the same target DNA concentration. In the inset graphs, greater linear relationships with the minus logarithmic values of the complementary target DNA concentrations ranging from 10^{-6} μM to 10^{1} μM have been clearly shown. Although in all these cases small shifts in the location of oxidation and reduction peaks after hybridization are observed, these changes can be served as a robust sensor readout signals. Curves in Fig. 5 strikingly illustrate that the well-regulated gradual changes of anode peaks of CV and peak currents of DPV. In Fig. 5(A), the regression equation is Y=0.9607X+27.011 (X:−log [complementary target DNA], Y: anode peak current values) with a correlation coefficient (R) 0.9997. Controlled series experiments show that if hybridization with one-point mismatched sequence (shown in Fig. 5(B)), the regression equation is Y=0.8027+19.4271(X:−log[one-

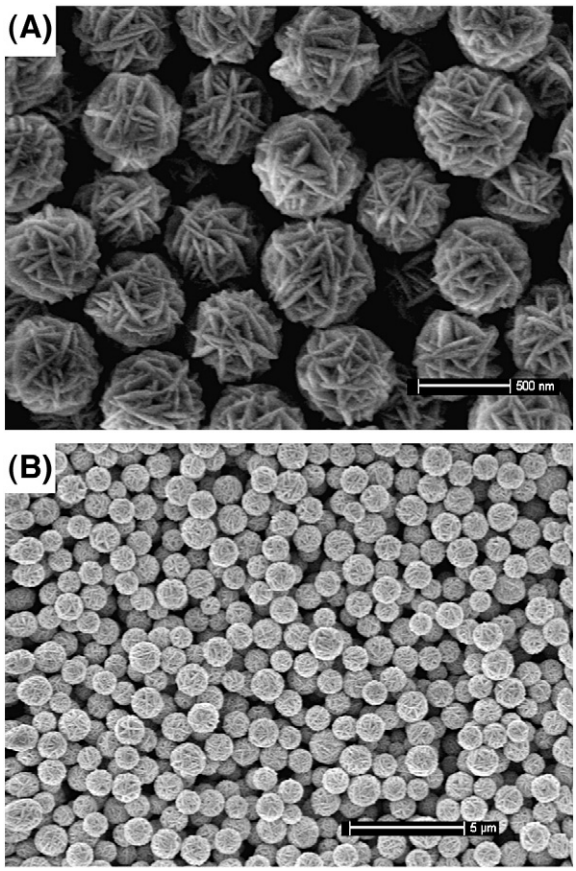

Fig. 2. SEM images of CdS crystals obtained under the dosage of PVP 0.12g/50 ml, the molar ratio of $CdCl_2$•2.5H_2O/$Na_2S_2O_3$•5H_2O=1:1, with reaction for 12 h at 160 °C. (A) The scale is 500 nm;(B) The scale is 5 μm.

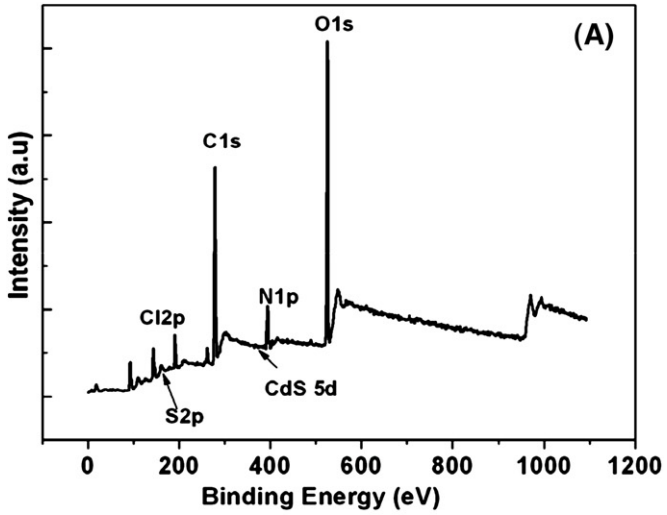

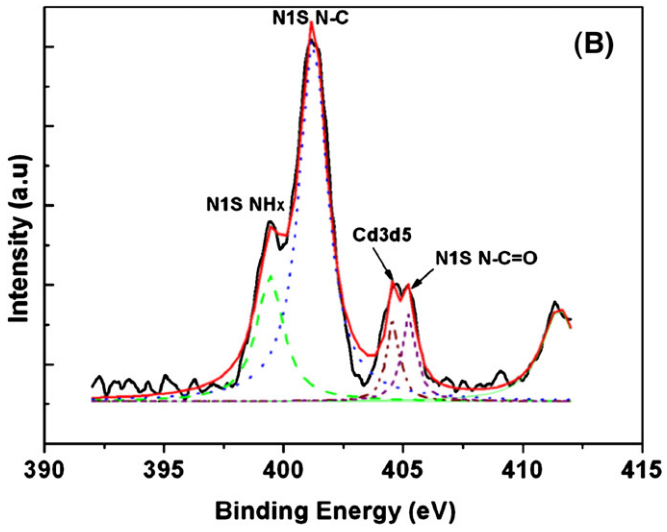

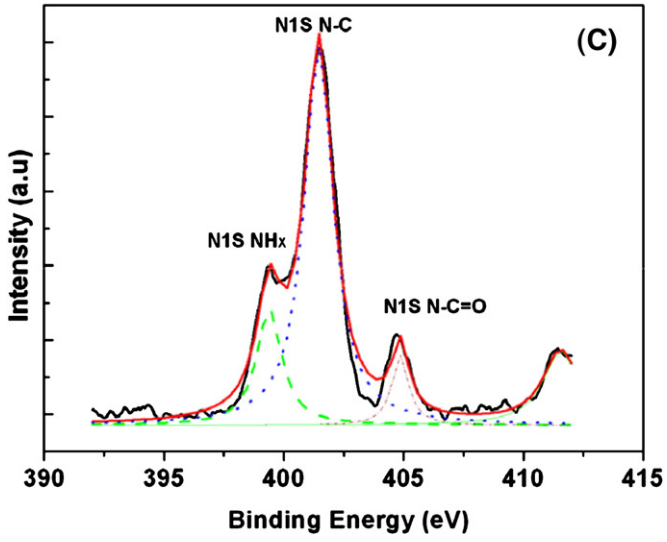

Fig. 3. (A) Wide scans of CdS modified silica (110) after DNA hybridization. (B) The N 1s region of the high-resolution XPS spectra acquired for the silica substrate after CdS surface modification step before DNA hybridization. (C) The N 1s region of the high-resolution XPS spectra acquired for the silica substrate after CdS surface modification step after DNA hybridization. All the data fit to multi-peaks Lorentzian approximation.

point mismatched target DNA], *Y*: anode peak current values) with a correlation coefficient (*R*) 0.966 and if hybridization with two-point mismatched sequence (shown in Fig. 5(C)) via Differential Pulse Voltammogram (DPV) method, the regression equation is $Y=0.2451X+1.4752$ (*X*:−log[two-point mismatched target DNA], *Y*: peak current values) with a correlation coefficient (*R*) 0.9943. Comparing the CVs signals of the completely complementary targets and the not completely complementary ones, the results demonstrate that the double standard helix covalently bonded to the CdS have more negative charges, space resistance for electron transference from buffer solution to GCE interface which causes the enhancements of sensor readouts. Based on these results, the sensor discriminates at a given target oligonucleotide concentration between fully complementary target, target with a single nucleotide mismatch and a mixture of them for the further research.

Table 1
XPS Elemental Surface Analysis of CdS-Capped GCE Nitride before and after the DNA hybridization

Surface XPS (at.%)	C1s			N1s			O1s	Cl2p	Cd3d5
	C–C	C–N	C–OH/COOH	N–H	N–C	NC=O/NH_3^+			
Immobilization probe DNA on the surface of CdS modified GCE	32.00	27.88	3.95	4.44	1.52	0.58	27.08	1.95	0.50
Probe DNA hybridization with complementary target	26.29	29.69	4.07	6.30	2.85	0.09	30.72	1.99	–

The selectivity of the CdS nanoparticles electrochemical hybridization assay was investigated by varying the kinds of CdS-ODN target (complementary, one-point mismatched sequences, two-point mismatched sequences) and the concentrations of each kind to hybridization with the probe ssDNA immobilized on the GCE shown in Fig. 6. The increase ratio of amplified signals modified with CdS is defined as (electrochemical signals from electrodes modified with CdS−signals from bare electrodes)/signals from bare electrodes×100%. Inset graphs indicate the absolute enhancement of signals defined as difference between electrochemical signals from electrodes modified with CdS and signals from bare ones. Under experimental condition mentioned before, the complementary sequence gives a more signi-

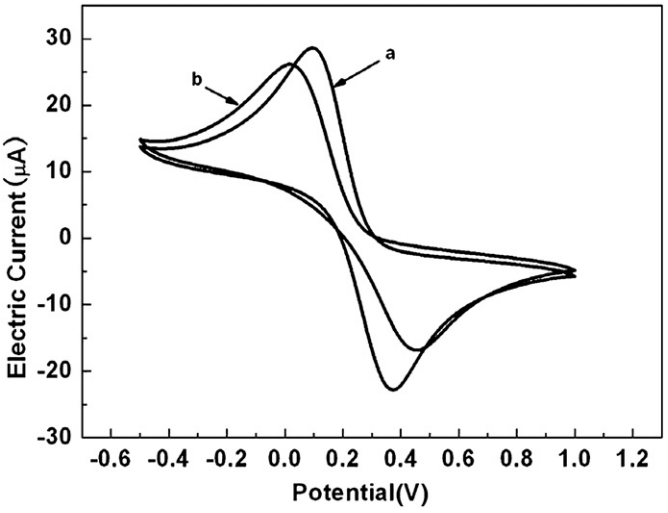

Fig. 4. Cyclic voltammograms of DNA hybridization detection with GCE modified with CdS nanoparticles (curve a), DNA hybridization detection with bare GCE (curve b) in a 0.1 M PBS buffer solution (with 0.1 M NaCl, pH 7.0) containing a 0.01 M K_3 [Fe $(CN)_6$] solution which seemed as a redox marker. The scan range from −0.5 V to 1.0 V (vs. Ag/AgCl) and scan rate 50 mV/s.The concentration of complementary target DNA is 0.01 μM and DNA hybridized under 20 °C for 2 h.

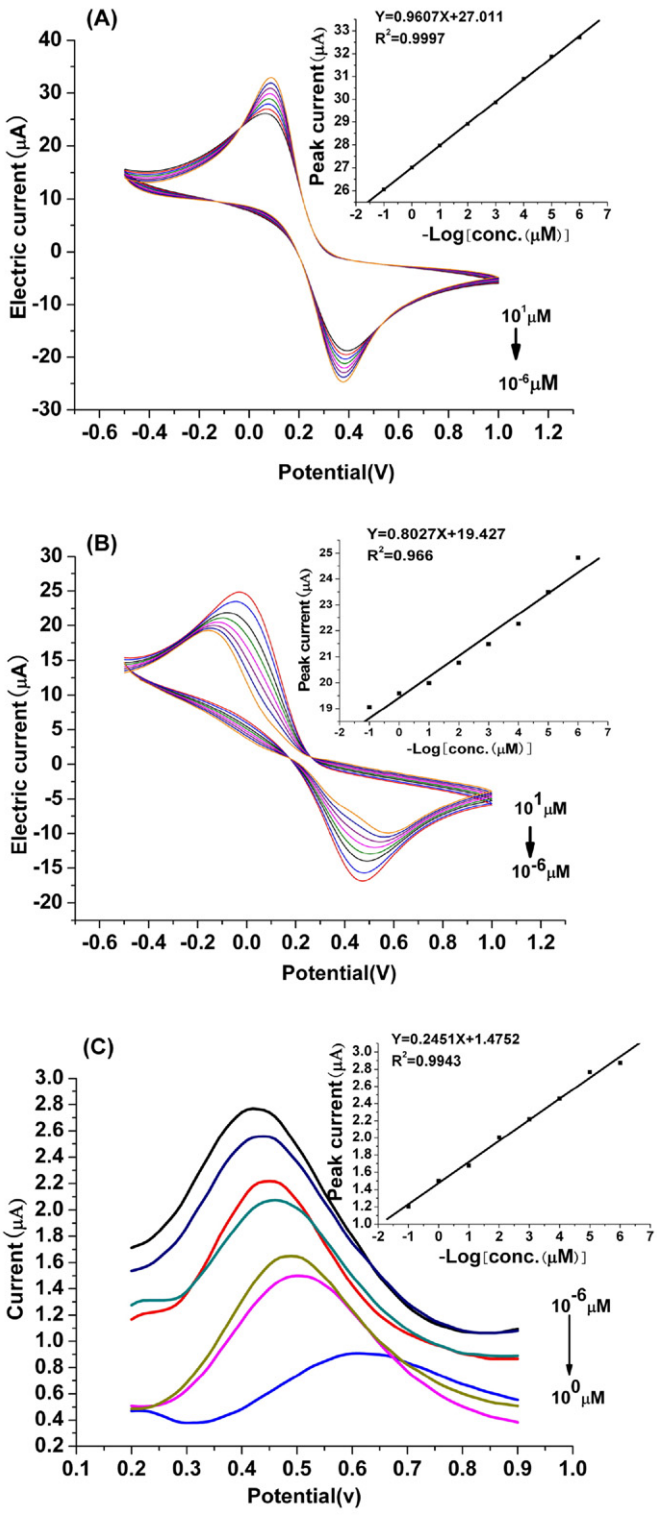

Fig. 5. CVs and DPVs of DNA hybridization detection with GCE modified with CdS nanoparticles by varying concentration of target DNA. The concentration of target DNA is from 10^{-6} μM to 10^{1} μM. Inset graphs show the linear correlation between the minus logarithm of concentration of target DNA and the peak currents. The three kinds of target DNA are: (A) complementary target DNA; (B) one-point mismatched target DNA; (C) two-point mismatched target DNA.

ficant response, following the one-point mismatched sequence. We conclude that both hybrid rate and the concentration of target DNA are the key factors for the CV signal detections because of their great influence on the number of transferred electrons per molecule of the

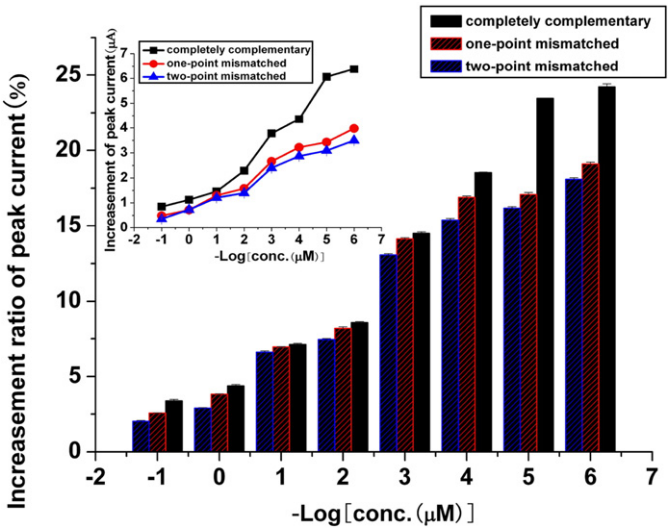

Fig. 6. The amplified CV peak current values of DNA hybridization on the surface of CdS modified GCEs comparing to the bare ones. The concentration of the three kinds of target DNA is from 10^{-6} μM to 10^{1} μM, respectively.

redox marker in the buffer solution. According to the equilibrium we deduce from Cottrell equation, Fick's law and Nernst equation:

$$i_p = 269\ A \bullet n^{3/2} \bullet D_R{}^{1/2} \bullet C_R^* \bullet v^{1/2} \quad (1)$$

$$i_p \propto n \quad (2)$$

where i_p is the current peak value, A is the electrode area (cm^2), D_R is diffusion coefficient corresponding to the electrode area ($cm^2\ s^{-1}$), C^*_R is the inner concentration of Red corresponding to the concentration of redox maker (mol dm^{-1}), v is the scan rate (V s^{-1}) and n is the number of transferred electrons through reaction interface per molecule of the redox marker in the buffer solution (mol^{-1}). From the equation, the current peak value is proportional to the number of transferred electrons per molecule of the redox marker in the buffer solution because the $AD_R^{1/2}C^*_R v^{1/2}$ value is treated as a constant in this paper. Considering about the concentration and the condense process of CdS nanoparticles, a near-complete layer of CdS-ODN nanoparticles covers the GCE surface before hybridization. The resulting interface has enhanced negative charged density compared to the bare GCE surface due to the additional charge of CdS nanoparticles. So a large electron-transfer barrier has formed because of the enhancement of the electrostatic repulsion of the negatively charged redox marker $[Fe(CN)_6]^{3-}$. Referring to the space resistance effect, the bulkiness of CdS-ODN and the double helix of hybrid DNA which have direct relationship with the concentration of target DNA provide a large hindrance for transferred electrons of redox marker $[Fe(CN)_6]^{3-}$ to access the electrode surface and finally contribute to the increase of the interfacial transfer. Generally speaking, the scope of the absolute amplified

Table 2
Comparing of the sensitivity and detection limit of GCEs modified with three kind of ODN targets and CdS-ODN targets in the process of DNA hybridization

Target DNA		Sensitivity(μA/log μM)	Detection limit (M)
Label-free target	Complementary	0.587	1.15×10^{-12}
	One-point mismatched	0.412	3.23×10^{-12}
	Two-point mismatched	0.384	6.78×10^{-12}
CdS-labeled target	Complementary	0.961	6.05×10^{-14}
	One-point mismatched	0.8027	9.51×10^{-14}
	Two-point mismatched	0.662	3.39×10^{-13}

anode peak values is from 1 to 7 μA. We attribute the trend of amplified signals shown in Fig. 6 that we get the best signal enhancement for the discriminations between complementary and mismatched target when the optimized target DNA concentration is 10^{-6} μM (increased by about 20%) and the amplified response values increase along with the dilution of target DNA buffers because of the integrated impacts of several effects discussed above.

3.5. Sensitivity, detection limit and stability of the sensor

Table 2 compares the estimated sensor detection limits based on the detectible CV signal changes of electrochemical current peak values using the following formula (3):

$$\text{Detection Limit (DL)} = 3.3\delta * S^{-1} \quad (3)$$

S is the slope of fitting regression line between the log [complementary target DNA] and anode peak current values, δ is the standard deviation of regression analysis and n is the times of repetitive experiments ($n=10$). The sensitivities obtained from the slopes of the regression of lines about the relationships of minus logarithm target concentrations and current anode peak values which come from DNA hybridization using CdS modified GCEs and bare GCEs, respectively. From the data in Table 2 we conclude that the use of CdS nanoparticle-labeled ODNs results in higher sensitivity and a significantly decrease in detection limit of the sensor (decrease by about 20 times each), which means the sensor will be able to discriminate between the complementary and mismatched target even when the concentration of target oligonucleotide is under 1 pM. This is due to several combined effects of hybridized CdS nanoparticles on the GCE surface. As reported previously, the larger size of nanoparticles comparing to the size of ODN and the negative surface charge of the capping layers hinder the access of the redox marker ($Fe(CN)_6^{3-}$) to the GCE surface and there increases the interfacial charge transfer resistance [13]. Meanwhile, the semiconductor nature of nanoparticles deposited on the surface by the hybridization event also increases the electron transfer resistance of conduction-band electron to the electrode by an electron hopping mechanism.

The stability of developed biosensor was evaluated by comparing the performance of CdS modified GCE in 20 CV and DPV recurrences respectively under the same experimental condition. The anode peak currents measured each time are no obvious deviation of that obtained in the first measurement. Meanwhile, the GCE modified with CdS nanoparticles which has DNA hybridization on its surface exhibited good stability. The peak currents measured on the seventh day are about 96.1% of that obtained in the first measurement.

4. Conclusions

The construction of a novel DNA sensor based on covalently bonded CdS nanoparticle-probe DNA conjugates on the electrode surface to amplify the readouts has been developed for DNA hybridization detection. An advantage of this sensor type resides on its simplified fabrication and no functionalized polypyrrole layer need to be synthesized during immobilization since the special walnut-like surface of CdS nanoparticles which can greatly increase the specific surface area to adsorb probes firmly on the surface of GCE. CdS nanoparticles trap more target sequences acting as a catalyzer of DNA hybridization. The X-ray photoelectron spectra study clearly demonstrates the surface modification steps and the feasibility of the as-prepared sensor for DNA hybridization detection. Significant amplification of concentration-dependence responses by the presence of CdS NPs is achieved in comparison with the use of CdS-unlabeled ODN probes via CV and DPV methods. The combined effects of semiconducting nature, superficial character of CdS nanoparticles and negative charges of CdS ligand attribute to the increase in interfacial charge transfer resistance of the negative charged redox marker $[Fe(CN)_6]^{3-}$, which has been explained for the mechanism of amplification. The resulting sensor shows great selectivity, high sensitivity, low detection limit and favorable stability among exact matches and mismatched sequences. The utility of combining two types of advanced materials to construct the nano-bio-conjugates is opening a brand new future for the direct recognizing of interactions between biomacromolecules in our further research.

Acknowledgements

The financial support of this work by the National Natural Science Foundation of China (project Nos. 60574095, 10635070), National High Technology Research and Development Program of China (Project NO. 2006AA03Z309), National Basic Research Program of China (2007CB936603) and The Knowledge Innovation Program of the Chinese Academy of Science are gratefully acknowledged.

References

[1] P.A.E. Piunno, U.J. Krull, R.H.E. Hudson, M.J. Damha, H. Cohen, Fiber optic biosensor for fluorimetric detection of DNA hybridization, Anal. Chim. Acta. 288 (1994) 205–214.
[2] Y. Okahata, Y. Matsunobu, K. Ijiro, M. Mukae, A. Murakami, K. Makino, Hybridization of nucleic acids immobilized on a quartz crystal microbalance, J. Am. Chem. Soc. 114 (1992) 8299–8300.
[3] C.E. Immoos, S.J. Lee, M.W. Grinstaff, Conformationally gated electrochemical gene detection, ChemBioChem. 5 (2004) 1100–1103.
[4] J. Wang, M. Jiang, A. Fortes, B. Mukherjee, New label-free DNA recognition based on doping nucleic-acid probes within conducting polymer films, Anal. Chim. Acta. 402 (1992) 7–12.
[5] S. Takenaka, K. Yamashita, M. Takagi, Y. Uto, H. Kondo, DNA sensing on a DNA probe-modified electrode using ferrocenylnaphthalene diimide as the electrochemically active ligand, Anal. Chem. 72 (2002) 1334–1341.
[6] K.M. Millan, Sequence-selective biosensor for DNA based on electroactive hybridization indicators, Anal. Chem. 65 (1993) 2317–2323.
[7] P.H. Dai, Aligned carbon nanotube–DNA electrochemical sensors, Chem. Commun. 3 (2004) 348–349.
[8] J. Wang, D. Xu, A.N. Kawde, R. Polsky, Metal nanoparticle-based electrochemical stripping potentiometric detection of DNA hybridization, Anal. Chem. 73 (2001) 5576–5581.
[9] J. Wang, G. Liu, A. Merkoci, Electrochemical coding technology for simultaneous detection of multiple DNA targets, J. Am. Chem. Soc. 125 (2003) 3214–3215.
[10] Y.C. Cao, R. Jin, C.A. Mirkin, Nanoparticles with Raman spectroscopic fingerprints for DNA and RNA detection, Science 297 (2002) 1536–1540.
[11] I. Willner, R. Baron, B. Willner, Integrated nanoparticle-biomelecule systems for biosensing and bioelectronics, Biosens. Bioelectron. 22 (2007) 1841–1852.
[12] H. Peng, C. Soeller, M.B. Cannell, G.A. Bowmaker, R.P. Cooney, J. Travas-Sejdic, Electrochemical detection of DNA hybridization amplified by nanoparticles, Biosens. Bioelectron. 21 (2006) 1727–1736.
[13] J. Travas-Sejdic, H. Peng, R.P. Cooney, G.A. Bowmaker, M.B. Cannell, C. Soeller, Amplification of a conducting poly-based DNA sensor signal by CdS nanoparticles, Curr. Appl. Phys. 6 (2006) 562–566.
[14] E. Palecek, F. Jelen, Electrochemistry of nucleic acids and development of DNA sensors, Crit. Rev. Anal. Chem. 32 (2002) 261–270.
[15] K. Kerman, M. Kobayashi, E. Tamiya, Recent trends in electrochemical DNA biosensor technology, Meas. Sci. Technol. 15 (2004) R1–R11.
[16] F. Lucarelli, G. Marrazza, A.P.F. Turner, M. Mascini, Carbon and gold electrodes as electrochemical transducers for DNA hybridization sensors, Biosens. Bioelectron. 19 (2004) 515–530.
[17] T. Livache, P. Guedon, C. Brakha, A. Roget, Y. Levy, G. Bidan, Polypyrrole electrospotting for the construction of oligonucleotide arrays compatible with a surface plasmon resonance hybridization detection, Synth. Met. 121 (2001) 1443–1444.
[18] M. Gerard, A. Malhotra, B.D. Malhotra, Application of conducting polymers to biosensors, Biosens. Bioelectron. 17 (2002) 345–359.
[19] Y. Xu, H. Cai, P.G. He, Y.Z. Fang, Probing DNA hybridization by impedance measurement based on CdS-Oligonucleotide nanoconjugates, Electroanalysis 16 (2004) 150–155.